Electronic Supplementary Information (ESI)

Chirality, Entropy and Crystallization in Polymers: Isotactic Poly(3-methyl-1-pentene) as Example of Influence of Chirality and Entropy on the Crystal Structure.

Claudio De Rosa,[a,*] Finizia Auriemma,[a] Chiara Santillo,[a] Rocco Di Girolamo,[a] Giuseppe Leone,[b] and Giovanni Ricci[b]

[a]Dipartimento di Scienze Chimiche, Università di Napoli Federico II, Complesso Monte S.Angelo, Via Cintia, I-80126 Napoli, Italy.
[b]CNR-Istituto per lo Studio delle Macromolecole (ISMAC), Via Bassini 15, I-20133 Milano, Italy.

Experimental details

Polymer synthesis

Samples of isotactic 1,2-poly(*E*-3-methyl-1,3-pentadiene) (iP3MPD12) have been prepared with the catalytic system $CoCl_2(PMePh_2)_2$/MAO as described in ref. S1. Toluene (total volume, 32 mL), (E+Z)-3-methyl-1,3-pentadiene (4 mL, 2.92 g), MAO (2.52 mL of toluene solution, 4×10^{-3} mol), and $CoCl_2(PMePh_2)_2$ (4×10^{-5} mol, as toluene solution) were introduced in this order in a 50 mL dried flask. The polymerization was terminated with methanol containing a little amount of hydrochloric acid after 120 h; the polymer was coagulated and repeatedly washed with fresh methanol and finally dried in vacuum overnight at room temperature (yield, 2.31 g).

Samples of the random copolymer iP(R,S)3MP of the two chiral monomeric units (R)3MP and (S)3MP have been prepared by hydrogenation of iP3MPD12 with diimide, produced *in situ* by thermal decomposition of p-toluenesulfonyl hydrazide (TSH),[S2] in boiling *o*-xilene as solvent. TSH (97%, Sigma-Aldrich) and *o*-xylene (Sigma-Aldrich, anhydrous grade) were used as received. The

hydrogenation reaction was carried out in a round-bottom flask equipped with a magnetic stirring, a reflux condenser, nitrogen inlet port and temperature controller. Typically, 2.20 g of iP3MPD12 were dissolved in 250 mL of xylene. The reaction mixture was kept under vigorous stirring at room temperature until the polymer was completely dissolved. TSH (16 g, 8.59×10^{-2} mol) was then added and the mixture was refluxed at 140°C. Further amounts of TSH (16 g, 8.59×10^{-2} mol) were successively added after 24h and 48h. Upon completion of the reaction after 72 h, the hot suspension was filtered, the solution obtained was reduced in volume, and the dissolved hydrogenated polymer was precipitated and coagulated by addition of methanol. The precipitated polymer was collected by filtration, then dried under vacuum at room temperature overnight. The polymer obtained was treated with boiling acetone through a Soxhlet method for 10 h in order to remove any excess TSH and products of the TSH decomposition. The residue to acetone extraction was dried under vacuum, then re-dissolved in hot toluene, successively precipitated with methanol, and dried under vacuum at room temperature to a constant weight (yield, 1.95 g of recovered polymer).

The molecular structures of the samples of iP3MPD12 and iP(R,S)3MP have been characterized by FT-IR, ^{1}H and ^{13}C-NMR, DSC and GPC analyses. Both samples iP3MPD12 and iP(R,S)3MP present high molecular mass (around 90000 g/mol) and are highly isotactic, with concentration of isotactic triad *mm* higher than 90%. Therefore, according to the synthetic strategy, the high isotacticity of iP3MPD12 ([*mm*] ≥ 90%) is preserved after hydrogenation.

X-ray Diffraction measurements

Unoriented films used for structural analysis have been obtained by compression molding of as-polymerized samples. The powders samples have been heated at ≈ 240 °C between perfectly flat brass plates under a press at very low pressure, kept at ≈ 240 °C for 5 min, and cooled to room temperature. Crystalline oriented fibers have been obtained by extrusion of melt in a syringe and stretching.

X-ray diffraction patterns have been obtained with Ni-filtered CuKα radiation (λ = 1.5418 Å). The powder diffraction profiles have been obtained with an automatic PANalytical X'Pert diffractometer operating in the Bragg-Brentano θ/2θ reflection geometry. A miniproportional PW3011 detector, mounted on the 2θ goniometer PW1050/37, has been used. The diffraction profiles have been recorded at room temperature and atmospheric pressure performing continuum scans of the diffraction angle 2θ in the range of 2θ = 3° - 50° at scanning rate of 0.02 deg/s. The powder samples are put in an Al sample holder 15 mm width, 20 mm length, 2 mm thickness and the measurements are performed in air. The diffraction intensity is recorded and integrated for a time of 5s within 2θ ranges of size of 0.1 deg. The diffraction profile is analyzed with the software X'PERT HighScore PLUS for the precise determination of the 2θ positions and intensity of the reflection peaks.

The X-ray fiber diffraction patterns have been recorded at room temperature and atmosphere pressure on a BAS-MS imaging plate (FUJIFILM) using a Huber cylindrical camera of radius of 57.30 cm and processed with a digital imaging reader Perkin Elmer Cyclone Plus (storage phosphor system). The fibers are mounted on a goniometric head and the measurements are performed in air. All the reflections observed in the powder diffraction profile of Figure 1a and fiber diffraction pattern of Figure 3 are listed in Table S1. The observed reflections are all accounted for by a monoclinic unit cell with parameters a = 10.02 Å, b = 18.48 Å, c = 6.87 Å and γ = 109.9°. The indices hkl of the reflections, according to this monoclinic unit cell, are also reported in Table S1. The unit cell has been determined and the reflections have been indexed with a graphical method of fitting the circles of radius equal to the cylindrical coordinate ξ of the reflections observed in the X-ray fiber diffraction pattern of Figure 3A (Table S1) with the nodes of the reciprocal lattice.

Table S1. Diffraction Angles (2θ), Bragg Distances (d), Cylindrical Reciprocal Coordinates (ξ and ζ) and Intensities (I_o) of the Reflections Observed on the Layer Lines l of the X-ray Fiber Diffraction

Pattern of iP(R,S)3MP of Figure 3A, compared with the Diffraction Angles, Bragg Distances, and Intensities Observed in the X-ray Power Diffraction Profile of Figure 1a. The Miller indices *hkl* of reflections for a monoclinic unit cell with parameters a = 10.02 Å, b = 18.48 Å, c = 6.87 Å and γ = 109.9° are also indicated.

Fiber diffraction pattern (Figure 3)							Powder diffraction profile (Figure 1a)			
2θ (deg)	d (Å)	ξ (Å^{-1})	ζ (Å^{-1})	l	I_o[a]	*hkl*	2θ (deg)	d_o (Å)	I_o	*hkl*
9.4	9.43	0.106	0	0	vs	100	9.3	9.51	41	100
10.2	8.69	0.115	0	0	vs	020	10.2	8.67	37	020
11.7	7.53	0.133	0	0	vw	$1\bar{2}0$	15.1	5.87	16	101
12.8	6.91	0.145	0	0	vw	110	16.4	5.40	35	021
16.8	5.28	0.189	0	0	vw	120	18.2	4.87	19	$1\bar{2}1, 2\bar{2}0$
18.1	4.89	0.204	0	0	vvw	$2\bar{2}0$	18.8	4.72	15	200
18.9	4.70	0.213	0	0	w	200	21.2	4.19	21	121
20.5	4.34	0.230	0	0	vw	040	22.1	4.02	12	201
25.3	3.52	0.284	0	0	vvw	140				
26.3	3.39	0.295	0	0	vvw	$3\bar{2}0$				
15.6	5.70	0.098	0.1456	1	w	101				
16.6	5.34	0.117	0.1456	1	s	021				
18.3	4.85	0.146	0.1456	1	w	$1\bar{2}1$				
21.2	4.20	0.188	0.1456	1	vw	121				
22.0	4.03	0.201	0.1456	1	w	201				

Conformational energy calculations.

The calculations of the conformational energy have been performed on a portion of isolated chains of iP(R)3MP, iP(S)3MP and iP(R,S)3MP shown in Figure S1, by application of the equivalence principle[S3] to successive constitutional units and assuming a line repetition symmetry group **s**(M/N) for the polymer chain. As a consequence, the sequence of the torsion angles in the main chain is of the kind ...$\theta_1\theta_2\theta_1\theta_2$... (Figure S1). The application of the constraints imposed by the equivalence principle and the assumption of the helical symmetry **s**(M/N) allow calculating the conformational energy of an isolated chain

molecule in the crystal field. The conformation of the chain found under this constrains generally corresponds to the conformation assumed by the chains in the crystal.[S3]

The intramolecular conformational energy has been calculated with the methods of molecular mechanics[S3,S4] using a consistent force field developed by Flory[S4] and suitable for polymer molecules. The energy has been calculated as the sum of three terms:

$$E = \sum_{b} E_b + \sum_{t} E_t + \sum_{nb} E_{nb}$$

where the bending E_b is the energy contribution due to deformation of bond angle () from the equilibrium value, which is assumed to have the form:

$E_b = (K_b/2)(-_o)^2$

the torsional energy E_t is the energy contribution associated with rotation around single bonds and is usually taken as a sinusoidal function of the torsion angle θ:

$E_t = (K_t/2)(1 + \cos 3\theta)$

and the non-bonded energy E_{nb} is the energy contribution due to the non-bonded interactions between atoms separated by more than two bonds, which is assumed to be the Lennard-Jones function:

$E_{nb}=A/r^{12}\ \ B/r^6$

The constants of bending, torsional and non-bonded energies of the used Flory force field[S4] are reported in Table S2.

The non-bonded energy has been calculated by taking into account the interactions between the atoms of the first monomeric unit and the interactions between these atoms and the remaining atoms within spheres having radii twice the van der Waals distances for each pair of atoms. The geometrical parameters assumed in the present calculations are reported in Table S3.

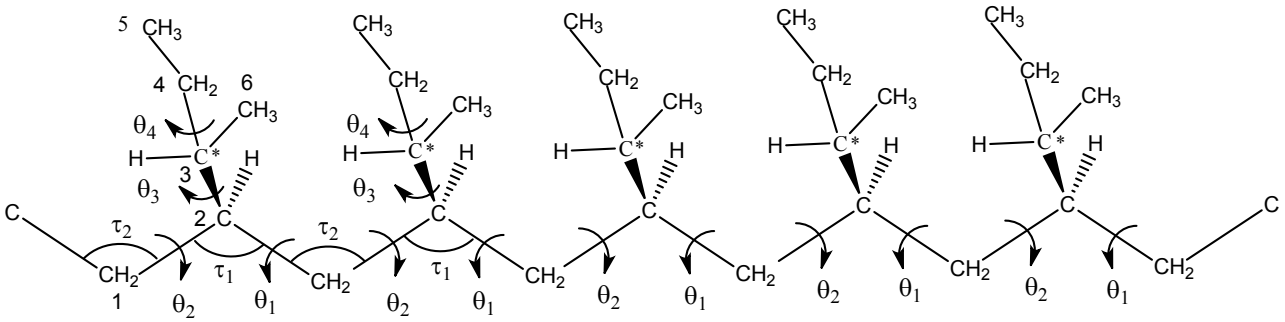

Figure S1. Portion of the chain of iP(S)3MP or iP(R)3MP used in the conformational energy calculations. The equivalence principle[S3] to successive constitutional units has been applied and a line repetition symmetry group **s**(*M*/*N*) for the polymer chain has been assumed. As a consequence, the sequence of the torsion angles in the main chain is ...$\theta_1\theta_2\theta_1\theta_2$... The definition of the torsion angles θ_1, θ_2, θ_3 and θ_4 and the bond angles τ_1 and τ_2 is shown. The torsion angle θ_3 is defined with respect to the carbon of the CH_2 group of the ethyl group: θ_3 = C4-C3*–C2-C1. The torsion angle θ_4 is defined with respect to the methyl group of the ethyl group: θ_4 = C5-C4–C3*-C2.

The calculations have been performed with a home-made software by calculating first maps of the internal energy as a function of the two torsion angles θ_1 and θ_2 (Figure S1) using the Flory force field,[S4] keeping bond lengths and bond angles constant at the values reported in Table S3. These calculations allowed finding all possible minima of conformational energy compatible with the constraints of the equivalence principle. Then, starting from the values of θ_1 and θ_2 corresponding to the energy minima found in the maps, the conformation has been optimized by minimization of the energy using the smart minimizer tool of the software package[S5] CERIUS[2] and using the force field PCFF.[S6] A cutoff distance of 4Å for attractive nonbonded interactions was selected and a spline function was used from 4 to 5 Å to attenuate gradually the interaction energy from its full value to zero. No interaction over 5Å was taken into account. We checked that similar results have been obtained using other force fields, for example the COMPASS force field.[S7]

Table S2. Parameters of the potential functions of the Flory force field used in the conformational and packing energy calculations.[S4]

Torsion angles	K_t **(kJ/mol)**	
C-C–C-C	11.7	
Bond angles	K_b **(kJ·mol^{-1}·deg^{-2})**	τ_o **(deg)**
C-C-C	0.184	109.47
C-C-H	0.121	109.47
H-C-H	0.100	109.47
Non-bonded interacting pairs	$A\times10^{-3}$**(kJ·mol^{-1}·Å^{12})**	B **(kJ·mol^{-1}·Å^{6})**
C-C	1654.5	1520
C-H	235.8	531
C-CH_3	4021.8	2671
H-H	30.2	196
H-CH_3	613.6	950
CH_3-CH_3	9671.8	4723

Table S3. Bond lengths and bond angles used in the conformational energy calculations of iP(S)3MP and iP(R)3MP.

Bond Length (Å)	
C-C	1.53
C-H	1.10
Bond Angles (deg)	
C'-C"-C'	113
C"-C'-C"	111
C"-C'-H	107.9
C'-C"-H	108.9
H-C"-H	108.0

[a]) C' indicates a methine carbon atom; C" indicates a methylene carbon atom.

Packing energy calculations.

Possible models of packing of 4/1 helical chains in the monoclinic unit cell with parameters a = 10.02 Å, b = 18.48 Å, c = 6.87 Å and γ = 109.9° have been found performing calculations of the packing energy for the space group $P2_1/b$. The chains have been positioned in the unit cell with their chain axes coincident with the crystallographic 2_1 axes of the space group $P2_1/b$. The packing energy has been calculated as half the sum of the interaction energies between the atoms of one monomeric unit and all the surrounding atoms of neighboring macromolecules. A cluster of 9 chains arranged on four neighboring monoclinic unit cells has been considered and the interaction energies between the atoms of the central chain of the cluster and all the surrounding atoms of the eight neighboring macromolecules

have been calculated. The lattice energy has been calculated as a function of the parameters ω and *z*, defined in Figure S2 and the conformation of the chain and the unit cell parameters have been kept constant. The calculations have been performed with a home-made software using a 6-12 Lennard-Jones potential with the constants of the force field reported by Flory *et al.*[S4] (Table S2) and taking the methyl groups as a single rigid unit. The interactions have been calculated within spheres of twice the sum of the van der Waals radii for each pair of atoms. Maps of the lattice energy as a function of ω and *z*, (Figure S2) using the Flory force field,[S4] have been first calculated. Then, starting from the values of ω and *z*, corresponding to the lattice energy minima found in the maps, the models of structure have been optimized by minimization of the lattice energy using the software package[S5] CERIUS[2] and using the force field PCFF.[S6]

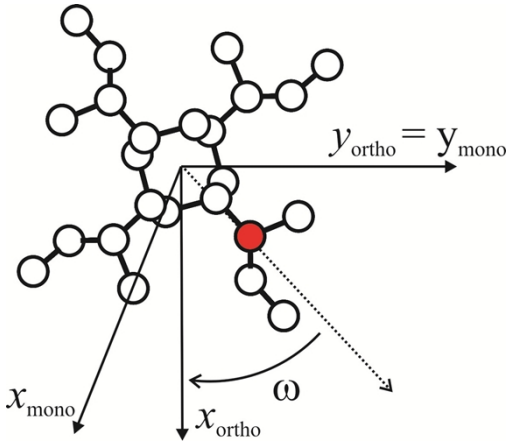

Figure S2. Definitions of the variables ω and *z* used in the packing energy calculations in the orthogonal (ortho) and monoclinic (mono) coordinates systems. The value of ω is positive for a clockwise rotation, and *z* is the height of the carbon atom indicated as a filled circle. The chain is positioned in the unit cell with its chain axis coincident with the crystallographic 2_1 axis of the space group $P2_1/b$ at fractional coordinate $x = 0$, $y = 0.25$.

Structure factors calculations

Structure factors have been calculated with a home-made software and compared to X-ray diffraction intensities evaluated from both X-ray powder diffraction profile and X-ray fiber diffraction patter.

Calculated structure factors have been obtained as $F_c = (\sum|F_i|^2 M_i)^{1/2}$, where F_i is the structure factor and M_i the multiplicity factor in powder or fiber diffraction[S3] of the reflection i (Miller indices $(hkl)_i$), and the summation is taken over all reflections included in the 2θ range of the corresponding diffraction peak observed in the X-ray powder diffraction profile or of the diffraction spot observed in the X-ray fiber diffraction pattern. A thermal factor B = 8 Å^2 and atomic scattering factors as in ref. S8 have been assumed.

The observed structure factors, F_o, have been evaluated from the intensities I_o of the reflections observed in the powder diffraction profiles or in the fiber diffraction pattern as $F_o = (I_o/LP)^{1/2}$, where LP is the Lorentz-polarization factor for X-ray powder diffraction,[S3] $LP = (1+\cos^2 2\theta)/(\sin^2\theta\cos\theta)$, or for X-ray fibre diffraction, $LP=(1 + \cos^2 2\theta)/[2(\sin^2 2\theta - \zeta^2]^{1/2}$, with the cylindrical coordinate $\zeta = \lambda l/c$, l and c being the order of the layer line and the chain axis, respectively, and λ the X-ray wavelength.[S3] The experimental intensities I_o have been evaluated from the powder diffraction profile by measuring the area of the peaks in the X-ray powder diffraction profile, after subtraction of a straight baseline approximating the background and of the amorphous contribution. For the amorphous profile the diffraction pattern of a sample of iP(*R*,*S*)3MP heat treated at high temperature was used. The experimental intensities I_o have also been evaluated from the X-ray fiber diffraction pattern by measuring the integrated intensity of spots recorded on the imaging plate I_{tot} upon subtraction of background intensity I_b, as $I_o = I_{tot} - I_b$. The background intensity I_b has been approximately evaluated by measuring the integrated intensity of regions placed around each spot free of Bragg contributions, having identical area of the spots.

Results of structure factors calculations for the space group $P2_1/b$ are reported in Tables S4 and S5. Comparison between observed structure factors (F_o), evaluated from the X-ray powder diffraction profile of Figure 1a and the fiber diffraction pattern of Figure 3A and structure factors calculated (F_c) for the limit disordered models of Figures 5A and B for the space group $P2_1/b$, are shown in Tables S4 and S5, respectively.

Simulated X-ray powder diffraction profiles and fiber diffraction patterns have been obtained with the software package[S5]CERIUS[2], using the isotropic thermal factor B = 8 Å^2. For the calculation of powder diffraction data, profile functions having a half-height width regulated by the average crystallite size along a, b, and c axes, $L_a = L_b$ = 200 Å and L_c = 150 Å, respectively have been used. These values correspond to a coherence length along a, b, and c and is not a true crystallite size. Simulated X-ray fiber diffraction patterns have been obtained fixing the half-width at half-height of crystallite orientation distribution (taken to be a Gaussian function centered on the fiber axis) equal to 9.13°. Structure factors calculations and simulated X-ray powder diffraction profiles and fiber diffraction patters have been performed for the models of packing found in the packing energy calculations and the final proposed disordered models of packing of Figure 5 have been found by trial and error method and no Rietveld refinement has been performed.

Table S4. Comparison between observed structure factors $F_o = (I/LP)^{1/2}$, evaluated from the intensities I observed in the X-ray powder diffraction profile of iP(*R*,*S*)3MP of Figure 1a, and calculated structure factors, $F_c=(\Sigma|F_i|^2M_i)^{1/2}$, for the limit disordered models of packing of Figures 5A and B of the random copolymer iP(*R*,*S*)3MP in the monoclinic unit cell with axes a = 10.02 Å, b = 18.48 Å, c = 6.87 Å and γ = 109.9° according to the space group $P2_1/b$.[a]

hkl	$2\theta_o$ (deg)	$2\theta_c$ (deg)	d_o (Å)	d_c (Å)	$F_o= (I_o/LP)^{1/2}$	$F_c=(\Sigma\|F_i\|^2M_i)^{1/2}$	
						Model of Figure 5A	Model of Figure 5B
100	9.34	9.39	9.47	9.42	87	84	85
020	10.19	10.18	8.68	8.69	91	109	96
$1\bar{2}0$	–	11.26	–	7.86	–	42	54
011	–	13.86	–	6.39	–	–	–
$1\,\bar{1}\,1$	15.14	15.75	5.85	5.62	89	–	–
101		15.96		5.55		94 } 97	91 } 97
120		16.06		5.52		24	35
021	16.36	16.45	5.41	5.39	142	130	139
$1\bar{2}1$	18.16	17.14	4.88	5.17	117	110	104
111		17.72		5.00		– } 141	– } 126
$2\bar{2}0$		18.11		4.90		89	70
200	18.74	18.84	4.73	4.71	109	64 } 78	63 } 74
$1\bar{4}0$		19.37		4.58		44	40
$1\bar{3}1$	21.17	19.81	4.20	4.48	143	–	–
031		20.05		4.43		–	–
040		20.44		4.34		26 } 116	18 } 107
121		20.64		4.30		113	105
$2\,\bar{1}\,1$	22.13	22.00	4.02	4.04	116	–	–
$2\bar{2}1$		22.29		3.99		9	10
$2\bar{4}0$		22.63		3.93		38	45
201		22.89		3.88		58	66
$1\bar{4}1$		23.33		3.81		25 } 112	34 } 115
$2\bar{3}1$		23.73		3.75		–	–
041		24.24		3.67		63	52
131		24.33		3.66		–	–
220		24.37		3.65		55	53
211	–	24.85	–	3.58	–	–	–
140	–	25.33	–	3.52	–	36	34
002	–	25.94	–	3.43	–	6	6
$2\bar{4}1$	–	26.13	–	3.41	–	11	7

012	–	26.45	–	3.37	–	–	–
$3\bar{2}0$	–	26.70	–	3.34	–	10	15
$1\bar{5}1$	–	27.41	–	3.25	–	–	–
$1\bar{1}2$	–	27.52	–	3.24	–	–	–
102	–	27.64	–	3.23	–	54	54
221	–	27.66	–	3.22	–	9	12
022	–	27.93	–	3.19	–	93	83
$1\bar{2}2$	–	28.36	–	3.15	–	42	29
300	–	28.42	–	3.14	–	52	52
141	–	28.52	–	3.13	–	58	49
112	–	28.72	–	3.11	–	–	–
051	–	28.79	–	3.10	–	–	–
$3\bar{4}0$	–	28.86	–	3.09	–	5	4
$1\bar{6}0$	–	29.01	–	3.08	–	61	58
$2\bar{5}1$	–	29.28	–	3.05	–	–	–
$3\bar{2}1$	–	29.75	–	3.00	–	15	18

[a]) The experimental Bragg angles ($2\theta_o$) and Bragg distances (d_o) observed in the X-ray powder diffraction profile of iP(*R,S*)3MP of Figure 1a and those calculated ($2\theta_c$ and d_c) for the monoclinic unit cell with axes a = 10.02 Å, b = 18.48 Å, c = 6.87 Å and γ = 109.9° are also reported.

Table S5. Comparison between observed structure factors $F_o = (I/LP)^{1/2}$, evaluated from the intensities I observed in the X-ray fiber diffraction pattern of iP(*R*,*S*)3MP of Figure 3A, and calculated structure factors, $F_c=(\Sigma|F_i|^2 \cdot M_i)^{1/2}$, for the limit disordered models of packing of Figures 5A and B of the random copolymer iP(*R*,*S*)3MP in the monoclinic unit cell with axes a = 10.02 Å, b = 18.48 Å, c = 6.87 Å and γ = 109.9° according to the space group $P2_1/b$.[a]

hkl	$2\theta_o$ (deg)	$2\theta_c$ (deg)	d_o (Å)	d_c (Å)	$F_o= (I_o/LP)^{1/2}$	$F_c=(\Sigma\|F_i\|^2 M_i)^{1/2}$	
						Model of Figure 5A	Model of Figure 5B
100	9.38	9.39	9.43	9.42	79	59	60
020	10.18	10.18	8.69	8.69	100	77	68
$1\bar{2}0$	11.75	11.26	7.53	7.86	26	29	38
110	12.80	12.11	6.91	7.30	24	–	–
120	16.78	16.06	5.28	5.52	31	17	25
$2\bar{2}0$	18.14	18.11	4.89	4.90	23	63	50
200	18.86	18.84	4.7	4.71	44	45	44
$1\bar{4}0$		19.37		4.58		31 } 55	28 } 52
040	20.47	20.44	4.34	4.34	33	18	13
$2\bar{4}0$		22.63		3.93		27 } 32	32 } 35
220	25.29	24.37	3.52	3.65	23	39	37
140		25.33		3.52		25 } 47	24 } 44
$3\bar{2}0$	26.28	26.70	3.39	3.34	10	7	10
300	–	28.42	–	3.14	–	37	36
$3\bar{4}0$	–	28.86	–	3.09	–	4	3
$1\bar{6}0$	–	29.01	–	3.08	–	44	41
$2\bar{6}0$	–	30.23	–	2.96	–	9	9
060	–	30.88	–	2.90	–	–	2
240	–	32.44	–	2.76	–	6	7
320	–	33.48	–	2.68	–	11	7
$3\bar{6}0$	–	34.23	–	2.62	–	12	9
011	–	13.86	–	6.39	–	–	–
$1\bar{1}1$	15.55	15.75	5.7	5.62	46	–	–
101		15.96		5.55		47 } 47	45 } 45
021	16.55	16.45	5.34	5.39	71	65	70
$1\bar{2}1$	18.30	17.14	4.85	5.17	52	55	52
111		17.72		5.00		–	–
$1\bar{3}1$		19.81		4.48		– } 55	– } 52
031		20.05		4.43		–	–
121	21.15	20.64	4.20	4.30	35	56	53

$2\bar{1}1$	22.00	22.00	4.04		–	–
$2\bar{2}1$		22.29	3.99		4	5
201		22.89	3.88		29	33
$1\bar{4}1$		23.33	3.81		12	17
$2\bar{3}1$		23.72	3.75	51	–	–
041		24.24	3.67		32	26
131		24.33	3.66		–	–
211		24.85	3.58		–	–
$2\bar{4}1$		26.13	3.41		6	3
$1\bar{5}1$	–	27.41	–	3.25	–	–	–
221	–	27.66	–	3.22	–	4	6
141	–	28.52	–	3.13	–	29	24
051	–	28.79	–	3.10	–	–	–
$2\bar{5}1$	–	29.28	–	3.05	–	–	–
$3\bar{2}1$	–	29.75	–	3.00	–	7	9
002	–	25.94	–	3.43	–	5	4
012	–	26.45	–	3.37	–	–	–
$1\bar{1}2$	–	26.52	–	3.24	–	–	–
102	–	27.64	–	3.23	–	27	27
022	–	27.93	–	3.19	–	46	42

[a]) The experimental Bragg angles ($2\theta_o$) and Bragg distances (d_o) observed in the X-ray fiber diffraction patter of iP(*R*,*S*)3MP of Figure 3A and those calculated ($2\theta_c$ and d_c) for the monoclinic unit cell with axes a = 10.02 Å, b = 18.48 Å, c = 6.87 Å and γ = 109.9° are also reported.

References.

S1) G. Ricci, G. Leone, A. Boglia, F. Bertini, A. C. Boccia, L. Zetta, *Macromolecules* 2009, **42**, 3048.

S2) H. J. Harwood, D. B. Russel, J. J. A. Verthe, J. Zymonas, *Die Makromol. Chem.* 1973, **163**, 1. L. A. Mango, R. W. Lenz Zymonas, *Die Makromol. Chem.* 1973, **163**, 13.

S3) C. De Rosa, F. Auriemma, *Crystals and Crystallinity in Polymers* Wiley: Hoboken, 2014.

S4) D Y. Yoon, P. R. Sundarajan, P. J. Flory, *Macromolecules* 1975, **8**, 765. D. Y. Yoon, P. R. Sundararajan, P. J. Flory, *Macromolecules* 1975, **8**, 776. P. R. Sundararajan, P. J. Flory, *J. Am. Chem. Soc.* 1974, **96**, 5025.

S5) *Cerius*^{2} *Modeling Environment*, Molecular Simulations Inc., San Diego, CA, 1999.

S6) a) U. Dinur, A. T. Hagler, "New Approaches to Empirical Force Fiels" in *Review of Computational Chemistry*, Chap. 4, 1991. b) J. R. Maple, U. Dinur, A. T. Hagler, *Proc. Nat. Acad. Sci. USA* 1988, **85**, 5350. c) H. Sun, S. J. Mumby, J.R. Maple, A. T. Hagler, *J. Am. Chem. Soc.* 1994, **116**, 2978; d) H. Sun, *Macromolecules* 1994, **26**, 5924. e) H. Sun, *Macromolecules* 1995, **28**, 701.

S7) a) H. Sun, D. Rigby, *Spectrochimica Acta* (A), 1997, **53**, 1301. b) D. Rigby, H. Sun, B. E. Eichinger, *Polymer International*, 1997, **44**, 311. c) H. Sun, P. Ren, J. R. Fried, *Computational and Theoretical Polymer Science*, 1998, **8** (1/2), 229. d) H. Sun, *J. Phys. Chem*. 1998, **102**, 7338.

S8) D. T. Cromer, J. B. Mann, *Acta Crystallogr.* 1968, **A24**, 321.